

Influence of Implant Connection Type on the Biomechanical Environment of Immediately Placed Implants – CT-Based Nonlinear, Three-Dimensional Finite Element Analysis

Roberto S. Pessoa, DDS, MS;* Luiza Muraru, MS;† Elcio Marcantonio Júnior, DDS, MS, PhD;* Luis Geraldo Vaz, MS, PhD;‡ Jos Vander Sloten, MS, PhD;† Joke Duyck, DDS, PhD;§ Siegfried V.N. Jaecques, MS, PhD§

ABSTRACT

Purpose: The purpose of the present study was to evaluate the biomechanical environment of immediately placed implants, before and after osseointegration, by comparing three different implant-abutment connection types.

Materials and Methods: A computer tomography-based finite element model of an upper central incisor extraction socket was constructed containing implants with either external hex, internal hex, or Morse-taper connection. Frictional contact elements were used in the bone, implant, abutment, and abutment screw interfaces in the immediately placed simulations. In osseointegrated simulations, the repair of bone alveolar defect and a glued bone-to-implant interface were assumed. By analysis of variance, the influence was assessed of connection type, clinical situation, and loading magnitude on the peak equivalent strain in the bone, peak von Mises stress in the abutment screw, bone-to-implant relative displacement, and abutment gap.

Results: The loading magnitudes had a significant contribution, regardless of the assessed variable. However, the critical clinical situation of an immediately placed implant itself was the main factor affecting the peak equivalent strain in the bone and bone-to-implant displacement. The largest influence of the connection type in this protocol was seen on the peak equivalent stress in the abutment screw. On the other hand, a higher influence of the various connection types on bone stress/strain could be noted in osseointegrated simulations.

Conclusions: The implant-abutment connection design did not significantly influence the biomechanical environment of immediately placed implants. Avoiding implant overloading and ensuring a sufficient initial intraosseous stability are the most relevant parameters for the promotion of a safe biomechanical environment in this protocol.

KEY WORDS: finite element analysis, immediate implant loading, immediate implant placement

*Department of Diagnostic and Surgery, Division of Periodontics, UNESP – São Paulo State University, Araraquara, Brazil; †Division of Biomechanics and Engineering Design, K.U. Leuven, Leuven, Belgium; ‡Department of Dental Materials and Prosthesis, Division of Dental Materials, UNESP – São Paulo State University, Araraquara, Brazil; §Department of Dentistry, Oral Pathology and Maxillo-Facial Surgery, BIOMAT Research Cluster, K.U. Leuven, Leuven, Belgium

Reprint requests: Dr. Roberto S. Pessoa, UNESP – Faculdade de Odontologia, Rua Humaitá, 1680, Sala 409 – Quarto Andar, Cep: 14802-550, Araraquara, São Paulo, Brazil; e-mail: rspessoa@uol.com.br

© 2009, Copyright the Authors

Journal Compilation © 2009, Wiley Periodicals, Inc.

DOI 10.1111/j.1708-8208.2009.00155.x

INTRODUCTION

In the last decade, promising results have been observed when nonsubmerged dental implants were subjected to immediate functional loads.¹⁻³ Immediate loading of implants offers several clinical benefits because both function and aesthetics are immediately restored. In some situations, this protocol has been associated to the immediate implant placement into fresh extraction sockets. This procedure reduces the treatment time and cost, decreases the number of surgical procedures, and optimizes the aesthetic results.^{4,5}

However, regardless of whether an implant is put in function after an undisturbed healing or immediately

after placement, the predictability and long-term success of implant treatment are greatly influenced by the biomechanical environment. The intimate bone-implant contact at the interface allows the direct transmission of the loads applied over the implant prosthetic device to the surrounding bone. The stress concentration can exceed the bone's tolerance level, can cause microdamage accumulation, and can induce bone resorption.⁶⁻⁸ Under certain conditions, this excessive occlusal loading may cause implant failure, even in osseointegrated implants.^{9,10} In addition, the bone supporting level is one of the most important factors for the maintenance of peri-implant aesthetic harmony because the bone level determines the peri-implant soft tissue position. Even if not progressive, marginal bone resorption in the buccal or proximal aspects of the implant can lead to recession or absence of papilla, respectively.^{11,12} In the immediate loading protocol, the overall requirement is to control interfacial movement between the implant and the surrounding bone. Micromovements that exceed 150 μm can induce fibrous connective tissue formation instead of the desirable bone regeneration.¹³⁻¹⁶

Some studies have demonstrated that the initial breakdown of the implant-tissue interface generally begins at the crestal region in successfully osseointegrated implants.^{6,7,9,10} Also, the majority of the mechanical failures occurs in the implant neck.¹⁷⁻²¹ Therefore, efforts have been made to evaluate the effects of different implant-abutment connections on the stress/strain distributions and magnitudes in the bone and in implant components. Merz and colleagues²⁰ compared, by experimental and finite element methods, the stresses induced by off-axis loads on tapered and butt-joint connections. They concluded that the tapered interface distributed the stresses more evenly when compared with the butt-joint connection. In another finite element study, Hansson²² observed that a Morse-taper implant-abutment at the level of the marginal bone substantially decreased peak bone stresses. Moreover, it improved the distribution of stress in the supporting bone. On the other hand, the shear stress was found to be located at the very top of the marginal bone, for a "flat-to-flat" implant-abutment interface. With a conical interface, the peak bone-implant interface shear stress had a more apical location, which could reduce marginal bone resorption.^{22,23}

There are already some experimental, numerical, and clinical studies²⁴⁻²⁶ evaluating the influence of implant-abutment connection on osseointegrated

implants. Nevertheless, there is limited information on many different outcome variables of immediately placed implants.²⁷ As well, no finite element (FE) studies were encountered on the biomechanical environment of dental implants placed into a fresh extraction socket. The evaluation of the stress/strain and displacement of the prosthesis/implant/bone complex in this clinical situation could contribute to the insight into the impact of abutment connection design.

Therefore, the purpose of the present study is to evaluate the biomechanical environment of dental implants placed into extraction sockets, before and after osseointegration. The influence of external hex, internal hex, and Morse-taper connections on the strain in peri-implant bone and on the stability of implants and abutments was compared.

MATERIALS AND METHODS

The computer tomography (CT) images of a dry maxilla, provided by the Department of Anatomy of the Faculty of Odontology at Araraquara (São Paulo State University, São Paulo, Brazil), were taken by a Picker UltraZ[®] CT scanner (Picker International Inc., Cleveland, OH, USA) with a gantry tilt of 0°, at 120 kV acceleration voltage and 1 mA current. The projection data were exported using the Digital Imaging and Communication in Medicine file format. The data set had a voxel size of 0.391 \times 0.391 \times 1.000 mm and consisted of contiguous slices with respect to the Z-axis.

Bone segmentation and reconstruction of an upper central incisor extraction socket geometry were accomplished by thresholding within an image-processing software (Mimics[®] 9.11; Materialise, Haasrode, Belgium). As the interest in this study was on the biomechanical environment in the vicinity of the implant, only the relevant part of the maxilla was reconstructed. A reconstruction of the entire maxilla would have led to a larger finite element model, with unacceptably high computational costs.

The computer-aided design (CAD) solid models of conical 13-mm implants, with a 4.3-mm-diameter shoulder, abutments, and abutment screws were provided by the implant producer (Neodent, Curitiba, Brazil). Morse-taper abutment and abutment screw are one single piece.

First, one implant model was imported in Mimics and positioned 1-mm deep inside the extraction socket, in a central position, to a palatal direction. The

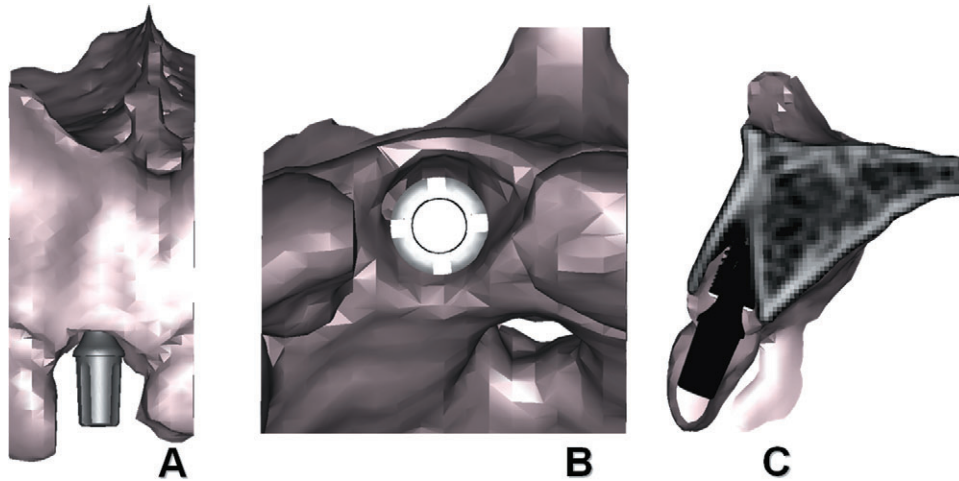


Figure 1 Implant positioned inside the extraction socket. *A*, Vestibulo-palatal view. *B*, Occlusal view. *C*, Proximal view.

contralateral teeth and the socket anatomy were used as a guide (Figure 1).²⁷

After having obtained the correct position of the implant, its inner part was removed and each implant-abutment connection was added. An external hex, an internal hex, and a Morse-taper implant with the very same external design and position were created. This procedure allowed having the same bone mesh and bone-implant interface for the three different implant-abutment connections. The implant insertion hole in the extraction socket solid model was obtained by means of Boolean subtraction.

The abutment and abutment screw models were then imported and aligned to the implant in their correct positions, following the instructions from the implant producer. No simplifications were made regarding the implant external and internal threads (ie, the spiral characteristic of the threads was maintained). However, the threads of the abutment screw CADs were edited to match perfectly the internal threads of the implants, to improve the contact status in this region. Second-order effects resulting from the tightening of the abutment and the preload in the abutment screw were not considered in the present study.

Bone, implants, abutments, and abutment screw models were meshed separately in MSC.Patran® 2005r2 (Figure 2) (MSC.Software, Gouda, the Netherlands).

A convergence study of the FE models was performed to verify the mesh quality. The convergence criterion was set to be less than 5% change of the peak von Mises stress (EQV stress) at the bone-implant edge.²⁸ In this region, the highest stress levels were encountered in

the first test analysis. These peaks were found to be in the same coordinates for all five mesh element sizes tested. The time of processing was also considered as an exclusion criterion in the study. Based on the result of the convergence study, the optimal global element size for bone mesh was 0.75 mm. Figure 3 shows the result for the convergence study. Tetrahedral meshes were constructed with different degrees of refinement for feature recognizing (ie, at threads). The smaller elements used were about 50 μm . Total number of elements and nodes in the models were an average of 110,000 and 15,000, respectively.

During meshing of the bone solid model, the entire volume that is contained within the outer bone surface was meshed. This means that the mesh consists of tetrahedral elements located in either cortical or trabecular bone. To discriminate between both tissues, different elastic properties were assigned, based on the gray values in the CT images.²⁹

The values of the Young's modulus and Poisson's ratio for the materials used in the present study were adopted from the relevant literature³⁰ and are summarized in Table 1.

For simulating the immediately placed implant, nonlinear, frictional contact elements (Coulomb frictional interface) were used. A friction coefficient μ of 0.3 was assumed between the bone and the implant.^{28,31} Between implant, abutment, and abutment screw regions in contact, a frictional coefficient of 0.5 was assumed.^{20,32} Frictional contact configuration allows minor displacements between all components of the model without interpenetration. Under these

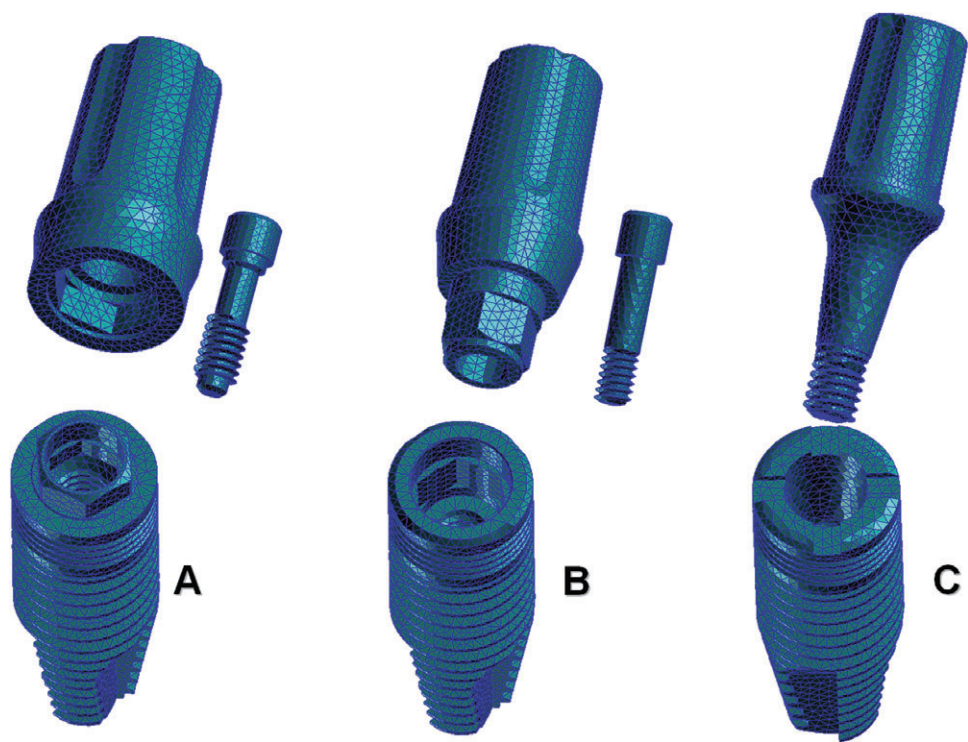


Figure 2 Implants, abutments, and abutment screws meshes. A, External hex. B, Internal hex. C, Morse taper. Note that the Morse-taper abutment and abutment screw are one single piece.

conditions, the contact zones transfer pressure and tangential forces (ie, friction), but no tension.

For simulating the stage after socket healing and implant osseointegration, the bone-implant interface

was assumed to be a bonded contact. In this configuration, no relative motion could occur at the bone-implant interface. In addition, a hard tissue bridge was modeled at the alveolar ridge region. The interface

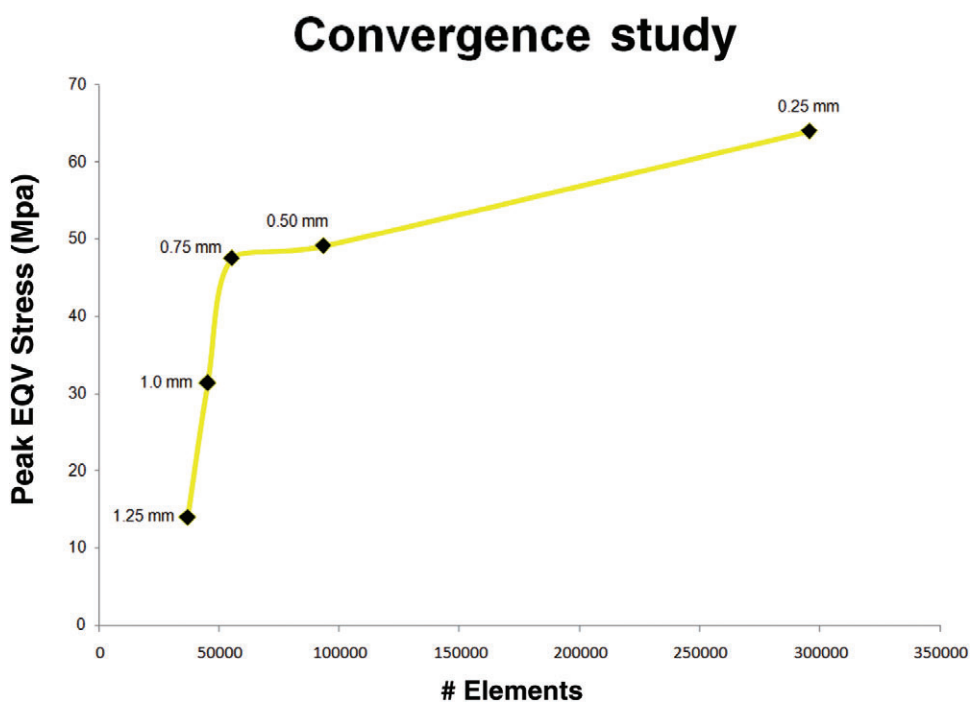


Figure 3 Influence of element size (1.25, 1.0, 0.75, 0.50, and 0.25 mm) on bone mesh density and peak equivalent (EQV) stress in bone model.

TABLE 1 Mechanical Properties of Bone, Implant, and Prosthetic Materials

Properties	Materials		
	Titanium	Cortical Bone	Trabecular Bone
Young's modulus (E) – MPa	110,000	13,700	1,370
Poisson's ratio (ν)	0.33	0.30	0.30

conditions for implant system components remained the same.

Models were fully constrained in all directions at the nodes on mesial and distal borders. A palato-buccal static load was applied as a point load centrally on the top of the abutment. The load inclination was 40 degrees in relation to the alveolus longitudinal axis. Loading magnitudes of 50, 100, and 200 N were adopted for both the immediately placed and osseointegrated simulations.^{33–35} The analysis and postprocessing were performed for each model by means of the MSC.MARC/Mentat® 2005r3 software (MSC.Software).

The data for peak equivalent strain (EQV strain) in the bone, bone to implant relative displacement, peak von Mises stress (EQV stress) in the abutment screw, and abutment gap were assessed and analyzed using a general linear model analysis of variance (ANOVA) (SAS/STAT® statistical software, version 9.1; SAS Institute, Cary, NC, USA). This procedure allowed calculating the percentage contribution of each of the evaluated parameters (connection type, clinical situation, and loading magnitude) and their interactions on the assessed results.³⁶

RESULTS

The EQV strain for the 100-N loading models was used to display the strain state in bone, for immediately placed simulations (Figure 4, A–F) and for osseointegrated simulations (Figure 5, A–F). The scale was set to range from 100 to 4,000 $\mu\epsilon$.³⁷ In Figures 4, A–C and 5, A–C, the implants were kept in order to make it easier to verify the influence of the strain transmission through the implant connection to the bone.

Data for EQV strain in the bone, bone-to-implant relative displacement, EQV stress in the abutment screw, and abutment gap are listed in Table 2. The EQV strains were also assessed in the implant median buccopalatal and mesiodistal paths in bone, 250 μm from the implant surface, for both 50-N loading immediately placed and

osseointegrated simulations (Figures 6 and 7). In addition, shear stress was assessed along the path in the implant median marginal buccal bone for the osseointegrated simulation (Figure 8).

The ANOVA results on the percentage contribution of the connection type, clinical situation, loading magnitude, and their interactions on the EQV strain in the bone, bone-to-implant relative displacement, EQV stress in the abutment screw, and abutment gap are shown in Tables 3–6, respectively.

Regardless of connection types, the highest strain concentration was seen at the buccal aspect of the peri-implant bone. Some high strains were also found at the outside of the ridge in both immediately placed and osseointegrated simulations. In immediately placed simulations, higher strain levels were seen for the Morse-taper connection, though in a more evenly distributed way, compared with the internal hex and external hex connections. External hex presented intermediate strain values, which were concentrated mostly in the buccal aspect of the bone. The lowest strain levels were seen for the internal hex. For this connection type, the strains were more evenly distributed than for the external hex. In a different way, for the osseointegrated simulation, external hex and internal hex showed similar strain levels, while Morse taper presented considerably lower strain values. Also in this clinical situation, the strain distribution was most even for the Morse taper, followed by internal hex and external hex, respectively. Strain distribution and values assessed in the bone paths followed almost the same pattern for all three connections. A greater influence of connection designs could be noted only for the marginal regions in the osseointegrated simulations. In this region, the peak shear stress was much higher for the external hex followed by the internal hex. These peak shear stresses for the external and internal hex were located at the very top of the marginal cortical bone. In a different way, for the Morse-taper connection, the shear stress was evenly distributed.

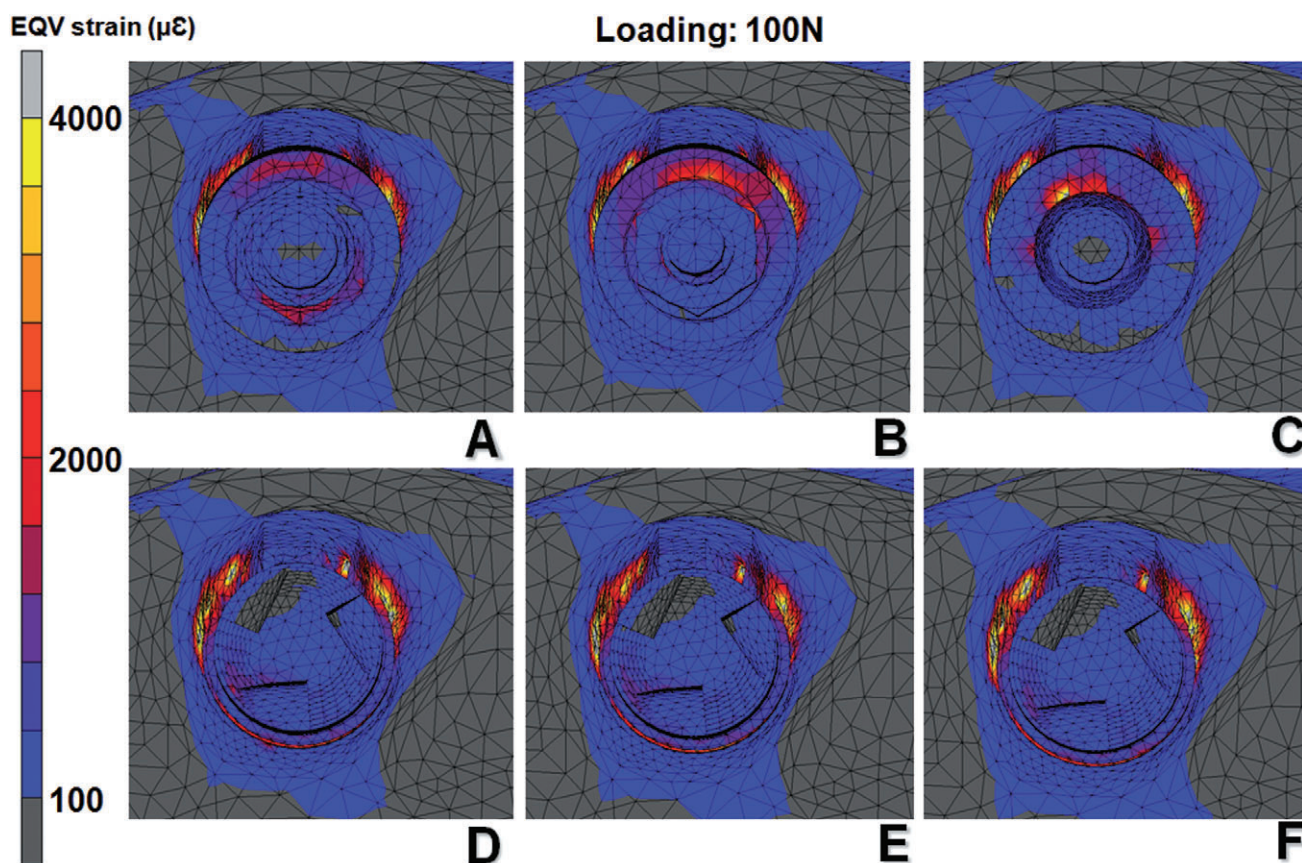


Figure 4 Occlusal view of equivalent (EQV) strain ($\mu\epsilon$) distribution for external hex (A and D), internal hex (B and E), and Morse taper (C and F) in the immediately placed simulations. Note that the implants were removed for clarity in parts D–F.

Regarding the bone-to-implant relative displacement in immediately placed simulations, the differences between the connection types were minor.

The von Mises stress (EQV stress) distribution in implant components is shown in a buccopalatal mesial plane in Figure 9, A–C. The stress is mostly concentrated in the abutment conical part in the Morse-taper connection. Minor EQV stress values were found in the implant and in the abutment screw. On the contrary, for external hex connection the major stress was concentrated in the abutment screw and in the implant region that remained in contact with the abutment. The same trend was seen for internal hex. However, comparing both connections, the external hex presented considerably higher stress concentration in the abutment screw than the internal hex.

Abutment stability was evaluated by means of the abutment vertical gap³⁸ in both immediately placed and osseointegrated simulations. However, it is important to emphasize that the gap reported in the present

study is because of the movement and deformation of the abutment as a direct consequence of the loading applied. It is related to the capability of the connection to provide stability. No preexisting misfit between implant and abutment, as is normally observed for internal hex and external hex connections,³⁸ was included in the model. The Morse-taper abutment showed the smallest gap. The internal hex was more stable and presented a smaller gap compared with the external hex. Comparing the clinical situations, abutment instability was higher in immediately placed simulations.

The percentage contributions of each parameter evaluated are presented in Tables 3–6. Regardless of the assessed result, the loading magnitudes have a significantly high contribution. The clinical situation has a greater contribution on the peak EQV strain in the bone and bone-to-implant displacement. The largest influence of the connection type was seen on the peak EQV stress in the abutment screw.

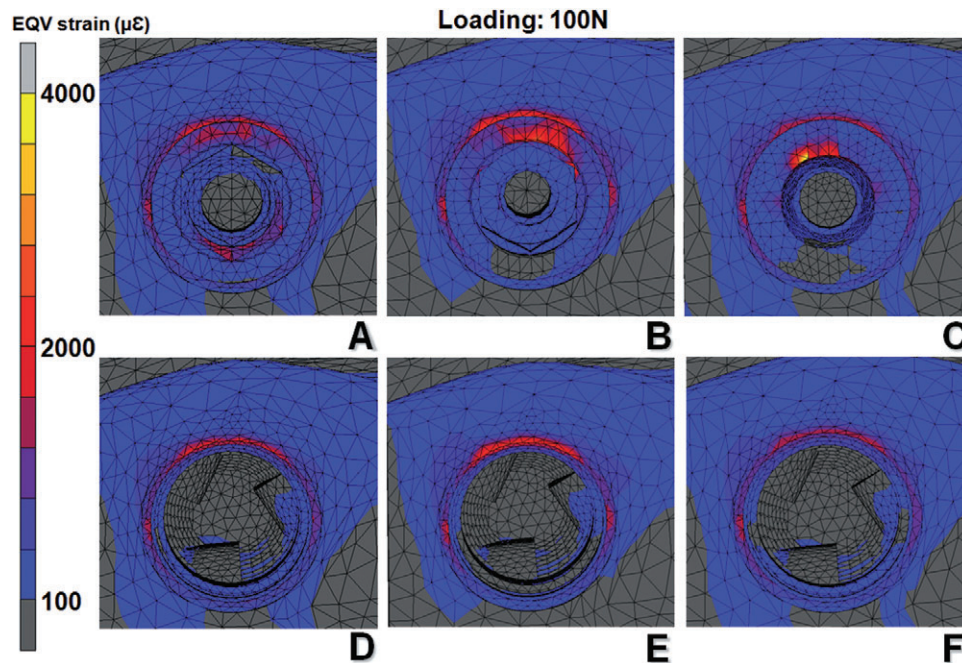


Figure 5 Occlusal view of equivalent (EQV) strain ($\mu\epsilon$) distribution for external hex (A and D), internal hex (B and E), and Morse taper (C and F) in the osseointegrated simulation. Note that the implants were removed for clarity in parts D–F.

DISCUSSION

The present finite element analysis (FEA) was carried out to evaluate the biomechanical environment of immediately placed and loaded implants. Morse-taper, internal hex, and external hex connections were compared. It was demonstrated that the implant-abutment connection design did not significantly influence the bone strain and the implant displacement of immediately placed implants. On the other hand, the Morse-taper connection presented superior abutment stability and the least stress concentration in the abutment screw. In the immediate implant placement protocol, sufficient initial intraosseous stability and a safe biomechanical environment, which avoids overloading, are the most relevant parameters on implant survival. Adverse forces over the implant-supported prostheses could not only cause abutment screw loosening and mechanical failures^{17–21} but could also impair osseointegration.^{6,7,9,10}

The immediately placed implant simulations showed slightly higher values of bone strain for the Morse-taper connection. On the contrary, the internal hex and external hex implants presented the lowest strain levels. These findings are in agreement with the results previously reported by Palomar and colleagues³⁹ in an FE study of an immediately loaded implant. Comparing rigid and resilient implant-abutment con-

nections, they found greater stress values in the bone for the rigid ones. A resilient component in the connection was shown to absorb some of the load, which resulted in a smaller stress in the bone for this kind of implant.³⁹ The connection type, however, had the lowest percentage contribution on the values of the peak EQV strain in the bone for immediately placed implants and was not statistically significant. The loading magnitude and the critical clinical situation of immediately placed implants were the major contributing factors for the bone strain in this protocol. Also, Hansson²³ observed that when the implant-abutment connection was positioned 2 mm coronally from the bone level, the effects of different connections were the same. In the present study, similar tendencies were observed in immediately placed implant simulations, probably because of the initial bone defect at the marginal region. This bone gap positioned the implant-abutment connections far from the bone.

On the other hand, the statistical analysis showed a significant contribution of the interaction between the connection type and the clinical situation on the EQV strain in the bone. It seems that the influence of the connection became higher by changing the clinical situation from immediately placed to osseointegrated. In osseointegrated models, the repair of bone alveolar defect and a glued bone to implant interface were

TABLE 2 Results for the Peak Equivalent Strain (EQV Strain) in the Bone, Peak Equivalent Stress (EQV Stress) in the Abutment Screw, Bone-to-Implant Relative Displacement (Displac.), and Abutment Gap for All Simulated Models

Connection Types	Clinical Situations	Loading (N)	Bone EQV Strain ($\mu\epsilon$)	Bone-Implant Displac. (μm)	Screw EQV Stress (MPa)	Gap (μm)
Morse taper	Immediately placed	50	4,997.8	5.1	57.3	4.5
	Osseointegrated	50	892.9	—	44.2	4.0
	Immediately placed	100	6,060.3	11.7	110.4	9.1
	Osseointegrated	100	1,817.0	—	89.1	8.1
	Immediately placed	200	9,910.1	24.4	225.0	18.4
	Osseointegrated	200	3,924.4	—	157.5	16.1
Internal hex	Immediately placed	50	3,762.4	5.3	76.5	6.0
	Osseointegrated	50	1,103.1	—	71.4	5.5
	Immediately placed	100	5,053.4	11.1	144.8	13.3
	Osseointegrated	100	2,593.5	—	128.6	11.6
	Immediately placed	200	9,048.2	23.3	350.7	27.3
	Osseointegrated	200	5,079.4	—	221.3	24.0
External hex	Immediately placed	50	4,013.7	5.5	124.4	8.0
	Osseointegrated	50	1,119.0	—	112.3	8.2
	Immediately placed	100	5,444.6	11.7	251.9	15.5
	Osseointegrated	100	2,232.8	—	224.1	15.5
	Immediately placed	200	10,209.8	24.0	495.0	31.2
	Osseointegrated	200	4,329.9	—	418.8	30.1

Immediate placement and loading

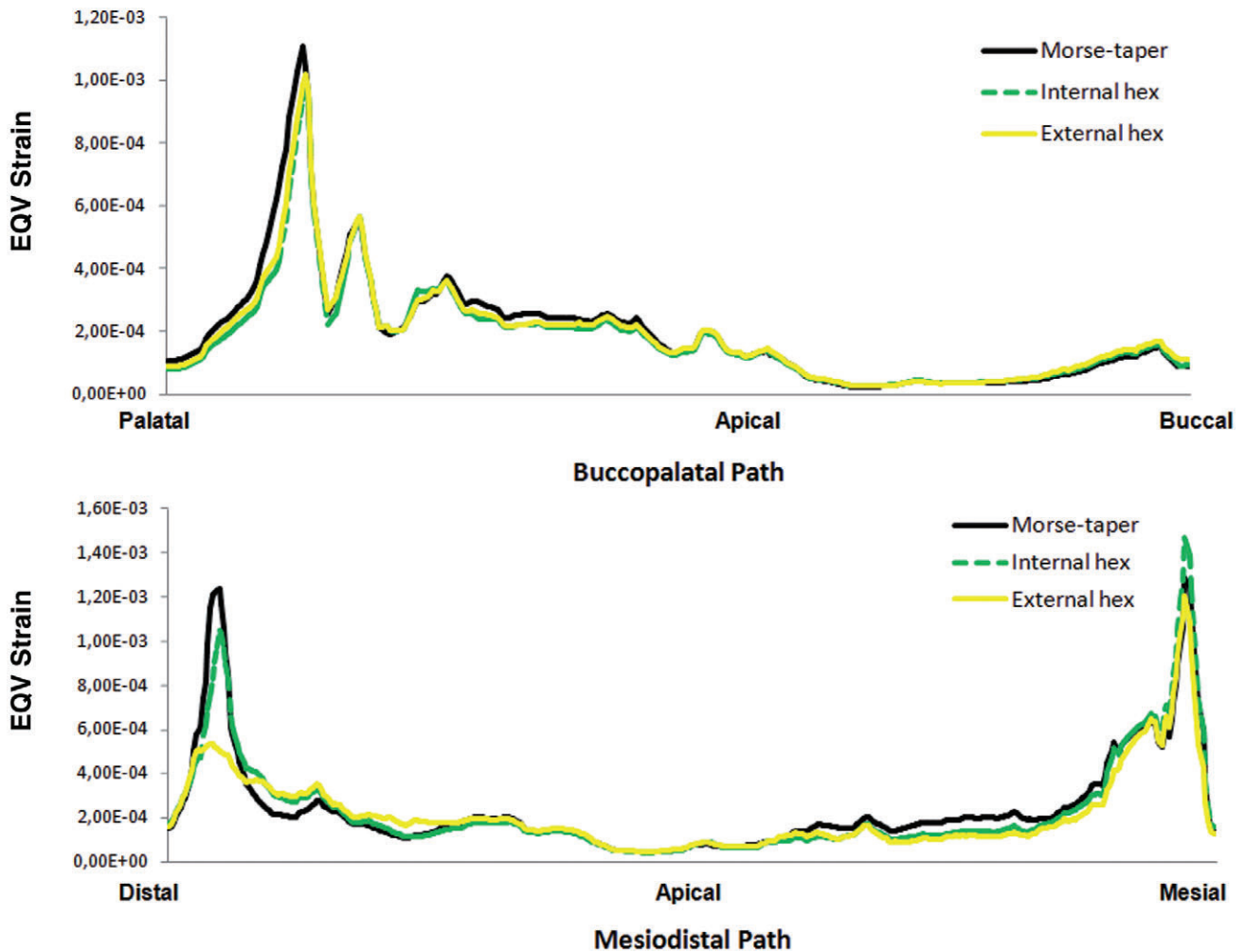


Figure 6 Equivalent (EQV) strains [-] assessed along a path in bone, 250 μm from implant-bone interface in the implant median buccopalatal and mesiodistal planes for 50-N loading immediately placed simulations.

assumed. In this way, the particular stress/strain distribution observed in each implant-abutment connection will result in different stress/strain patterns in the bone, mainly when the bone reaches levels close to the implant crest.²³ The results of the current FEA for the osseointegrated model are in accordance with the findings of Hansson.²³ Using FEA, Hansson²³ showed that a conical implant-abutment interface at the level of the bone crest decreases the peak bone-implant interfacial stress as compared with the flat top interface. For the conical implant-abutment interface, this peak interfacial shear stress was located at some depth in the marginal bone. For the flat top implant-abutment interface, the shear stress was located at the top marginal bone.^{22,23} In the present study, the shear stress assessed in a path in the

marginal buccal bone region also showed the same trend. Comparing the external and internal hex connections, a smaller amount of shear stress occurred at the cervical area for the internal configurations. This can be explained by the difference in surface area between connections. The conical interface of the Morse taper, as well as the lateral wall of the internal hex abutment, helped to dissipate the forces to the fixture.⁴⁰

Another interesting observation is the fact that some strain was encountered at the outside of the ridge for immediately placed implant simulations. Analogous results were observed by Cehreli and colleagues⁴¹ in a cadaver model. The authors argued that minimal load was transferred to the labial marginal bone because of the absence of direct contact with the implant, because

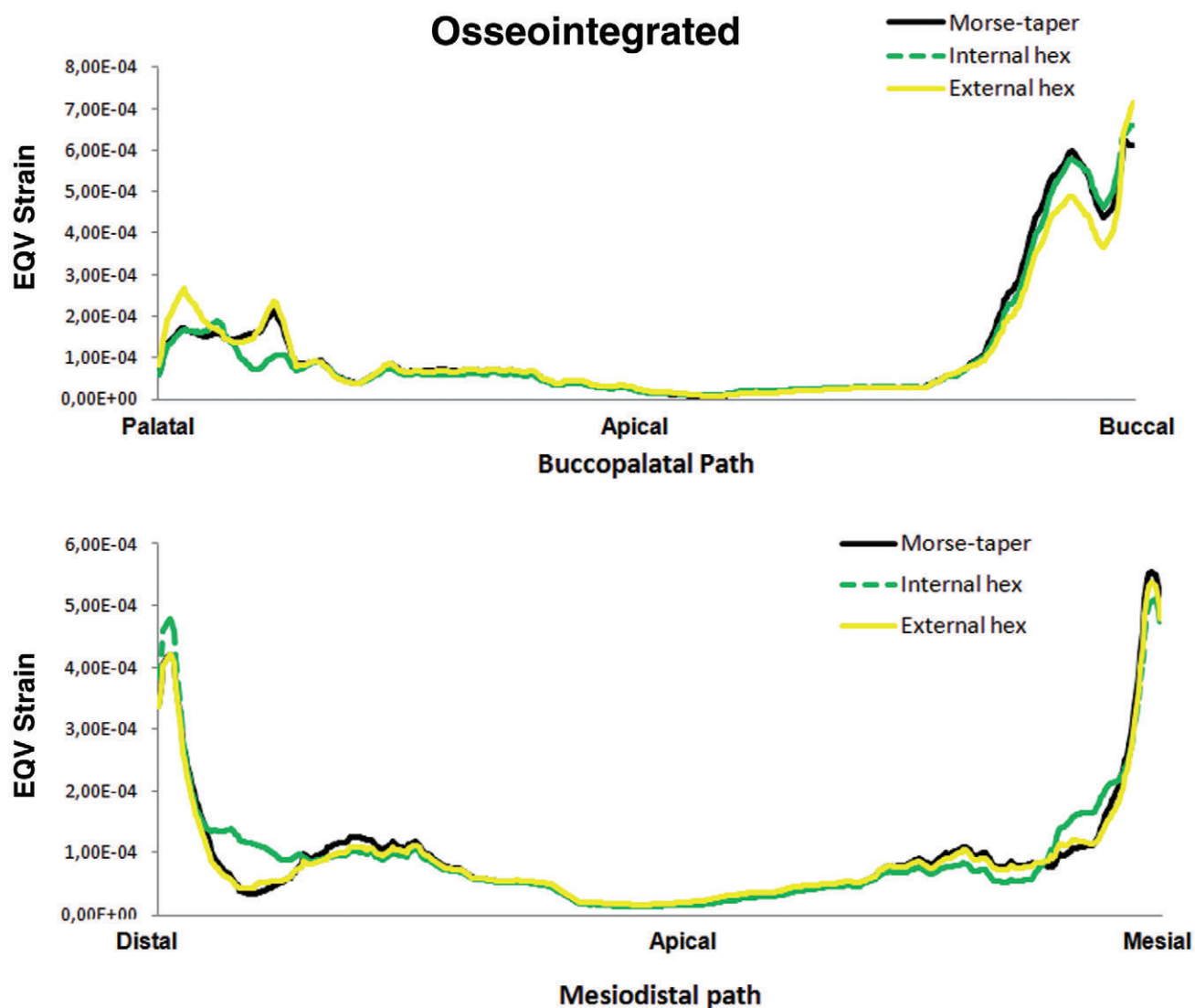


Figure 7 Equivalent (EQV) strains [-] assessed along a path in bone, 250 μm from implant-bone interface in the implant median buccopalatal and mesiodistal planes for 50-N loading osseointegrated simulations.

of the site-specific three-dimensional shape of the bone defect. However, in the real clinical situation, once an implant is immediately placed, the coagulum and thereafter the initial connective tissue in the bone defect could transfer functional load and stimulate the bone that is not contacting the implant.^{42,43} One can speculate whether such stimulus could avoid disuse atrophy of the marginal bone.^{3,44}

In the present FEA, to facilitate the visualization of the strain state in the bone, the scale was set to range from 100 to 4,000 $\mu\epsilon$. Frost⁴⁵ considered 4,000 μ strain as a possible threshold for pathologic bone overload. Also, Duyck and colleagues,⁶ by FEA based on CT images, estimated the value associated with overload-induced resorption as 4,200 $\mu\epsilon$. Nevertheless, although

the peak of bone strain exceeded 4,000 $\mu\epsilon$ for all implant connections in our immediately placed implant simulations, this does not necessarily imply bone overloading and implant loss. Rather than only strain amplitude, loading frequency and number of loading cycles are also parameters capable to greatly influence the cortical bone adaptive response.⁴⁶⁻⁵⁰ Furthermore, the loading applied in the present study was static, and bone responds to dynamic rather than to static loads.^{6,51-53} In this way, it must be clear that the modeling of bone adaptive processes was not one of the aims in the current FEA.

In addition, the peaks of strain appeared locally in a minor part of the marginal bone for 50- and 100-N loading magnitudes (see Figure 4, D-F), where indeed

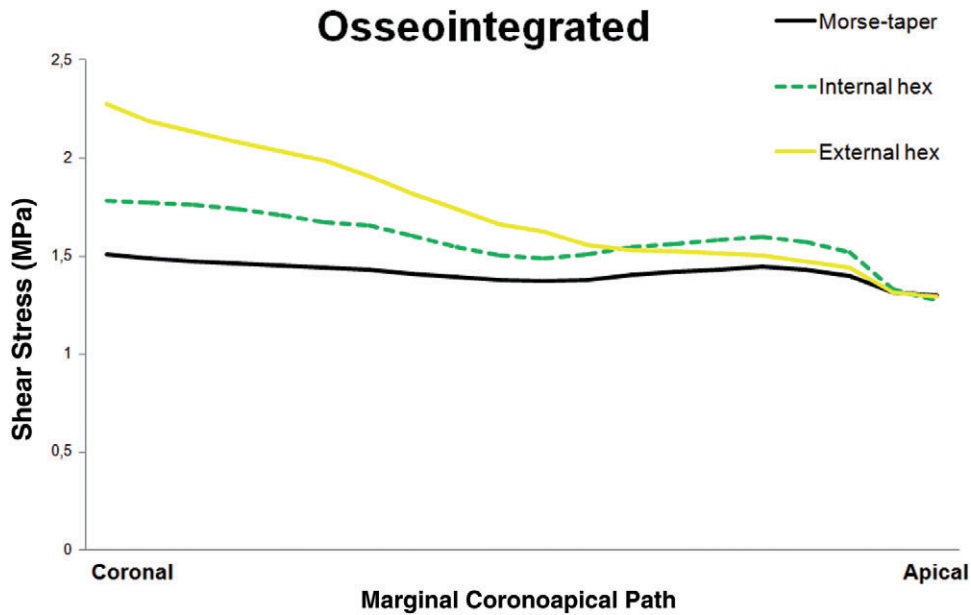


Figure 8 Shear stress (MPa) assessed along a path in marginal bone, 250 μm from implant-bone interface in the implant median buccopalatal plane for 50-N loading osseointegrated simulations.

some localized bone resorption is likely to occur.^{6,45} This statement is also corroborated by the strain values along paths in the bone for 50-N loading at 250 μm from the implant surface. The graphs showed peaks of strain lower than 1,200 $\mu\epsilon$, independently of implant connection, bone region, and clinical situation. The present

study focused only on the relative influence of implant connection type on bone strain values.

In essence, one of the most critical elements for an uneventful bone tissue formation around an immediately loaded implant is a stiff bone-implant interface, allowing low implant micromovement in the bone.^{16,54}

TABLE 3 Analysis of Variance for the Peak Equivalent Strain in the Bone					
Parameter	Degrees of Freedom	Sum of Squares	Mean Square	p Value	Contribution (%)
Connection type	2	83,004.42	41,502.21	0.6799	0.06
Clinical situation	1	69,652,650.49	69,652,650.49	<0.0001*	49.94
Connection type \times clinical situation	2	2,301,719.20	1,150,859.60	0.0210*	1.65
Loading magnitude	2	63,012,208.21	31,506,104.10	<0.0001*	45.18
Connection type \times loading magnitude	4	340,997.31	85249.33	0.5503	0.24
Clinical situation \times loading magnitude	2	4,068,982.43	2,034,491.22	0.0077*	2.92

p < .05.
*Statistically significant.

TABLE 4 Analysis of Variance for the Relative Displacement between Implant and Bone				
Parameter	Degrees of Freedom	Sum of Squares	Mean Square	Contribution (%)
Connection type	2	0.50	0.25	0.10
Loading magnitude	2	538.16	269.08	99.83
Connection type \times loading magnitude	4	0.44	0.11	0.08

Saturated experimental design; no p values were reported.

TABLE 5 Analysis of Variance for the Peak Equivalent Stress in the Abutment Screw

Parameter	Degrees of Freedom	Sum of Squares	Mean Square	p Value	Contribution (%)
Connection type	2	172.88	86.44	<0.0001*	29.16
Clinical situation	1	14.58	14.58	0.0031*	2.46
Connection type × clinical situation	2	1.25	0.63	0.2841	0.21
Loading magnitude	2	401.33	200.66	<0.0001*	67.69
Connection type × loading magnitude	4	0.38	0.10	0.8864	0.06
Clinical situation × loading magnitude	2	2.48	1.24	0.1338	0.42

p < .05.

*Statistically significant.

In the present study, all three connection types showed similar values of displacement ranging from 5 to 25 μm, for the immediately placed simulations. Though important differences exist regarding, for example, the implant designs, the clinical situations, and the loading magni-

tudes and directions, the results presented in the current study are in line with other FEAs of immediately loaded implants. Huang and colleagues²⁸ reported a maximum sliding distance of 12.5 μm between threaded implants and bone, for a 100-N force over an immediately loaded

TABLE 6 Analysis of Variance for the Abutment Gap

Parameter	Degrees of Freedom	Sum of Squares	Mean Square	p Value	Contribution (%)
Connection type	2	69.35	34.68	0.4758	6.95
Clinical situation	1	76.88	76.88	0.2308	7.70
Connection type × clinical situation	2	60.30	30.15	0.5168	6.04
Loading magnitude	2	589.43	294.72	0.0430*	59.04
Connection type × loading magnitude	4	88.75	22.19	0.6972	8.89
Clinical situation × loading magnitude	2	113.72	56.87	0.3312	11.39

p < .05.

*Statistically significant.

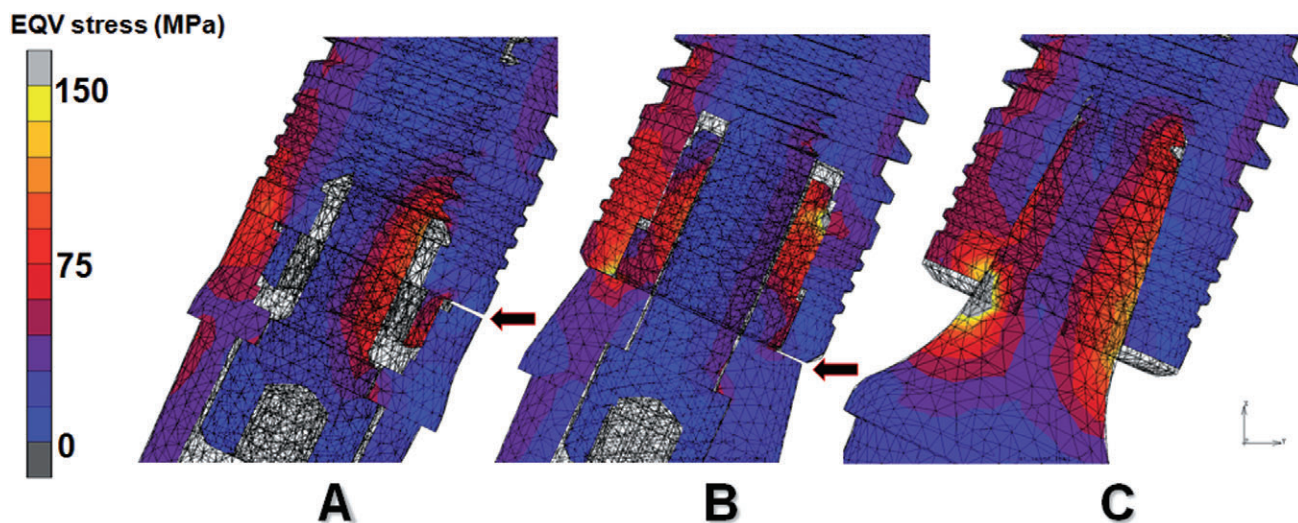


Figure 9 Equivalent (EQV) stress (MPa) distribution inside implant connections (A, external hex; B, internal hex; C, Morse taper). The deformation is 10-fold magnified for visualization. Note abutment gap as a result of the loading for the external hex and internal hex (black arrows).

maxillary implant. Comparing resilient and rigid abutments by an FEA of immediately loaded implants in a mandibular premolar region, Palomar and colleagues³⁹ found maximum vertical implant displacements of 12.67 and 12.47 μm , respectively. This difference in implant displacement is qualitatively similar to the one found in this study for internal hex (11.1 μm) and external hex (11.7 μm). However, as shown in the statistical analysis, the connection type did not significantly influence the bone to implant relative displacement.

The current FEA showed that the connection type has a significant contribution to the EQV stress in the abutment screw and to the abutment gap. In these parameters, Morse-taper implant presented a considerably lower EQV stress in the abutment screw and lower abutment gap values, in both simulated clinical situations. The internal hex presented the intermediate values and the external hex the highest connection instability. This observation corroborates data presented by Merz and colleagues,²⁰ who stated that a tapered connection is mechanically more stable than the butt-joint configurations. Also, Khraisat and colleagues,⁵⁵ using repeated loading, observed a significantly better fatigue strength for a tapered joint design, compared with an external hex connection. The reduced stress in the abutment screw and reduced gap observed for the Morse taper in the present study was probably provided by its superior joint stability.⁵⁶

The same factor could also be used to explain the differences in stress distribution among the three implant-abutment connections. Basically, the Morse-taper and the butt-joint configurations have quite different functional behavior. In a taper connection, the loading is resisted mainly by the taper interface. It prevents the abutment from tilting off, allowing stable retention of position by frictional forces.²⁰ Differently, an external hex configuration determines the rotational position, but there is no form or positive locking. In this way, the lateral loading is absorbed mainly by the abutment screw.²⁰ On the other hand, in an internal hex connection, the lateral wall of the abutment also helps to dissipate the lateral forces and protects the abutment screw from excessive stress. Substantially lower EQV stresses were observed in the internal hex abutment screw in the current FEA, compared with the external hex. Also, the bone-to-implant interface condition and the clinical situation have a significant contribution to

abutment stability. Slightly higher abutment stability and less EQV stress in the abutment screw were seen for the osseointegrated situation.

The intricate implant designs and their relationship with the supporting tissues and prosthetic restoration prevent the use of simple formulas to evaluate the effect of external loading on the internal stresses/strains and displacements. In this way, the FE method can offer some information unavailable from clinical or experimental studies.³⁰ In addition, numerical simulations permit the evaluation of possible explanations for in vivo and clinical findings, and also suggest directions for further investigations. Nevertheless, the results obtained in the present FEA should be interpreted with some care. It was not possible in this study to answer the question as to whether bone overload does actually occur in immediately placed implants. The answer to that question is indeed patient specific and requires a patient-specific finite element model that incorporates patient-specific bone anatomy, bone density distribution, implant position, and in vivo measured implant loads.⁵⁷ On the other hand, the statistical analysis on the FEA results allowed the assessment of the real relative effects of each investigated factor on the mechanical response of the bone and implant components in various clinical situations. The relevance of efforts to develop implant designs capable of providing a safe biomechanical environment, especially for the newer protocols of implant usage, is not disputed. However, varying the implant-abutment connection type was not able to significantly improve the biomechanical environment in the immediately placed implant protocol.

CONCLUSIONS

Within the limitation of this FE analysis, it can be concluded that:

1. different implant-abutment connection types do not significantly influence the biomechanical environment of immediately placed implants;
2. loading magnitude and the critical clinical situation of immediately placed implants itself are the main factors affecting the equivalent bone strain and implant displacement;
3. the Morse-taper connection provided the best abutment stability and the lowest von Mises stress concentration in the abutment screw compared with the internal hex and external hex connections;

- the effect of the various connection types on bone stress/strain may be higher for osseointegrated implants.

ACKNOWLEDGMENTS

The authors thank the Neodent® implant system for providing the implant CAD models. Dr. S. Fieuws from the Leuven Biostatistics and Statistical Bioinformatics Centre (L-BioStat) is acknowledged for the factorial design optimization and ANOVA analyses. Roberto Pessoa gratefully thanks the grants and scholarships from FAPESP (Research Support Foundation of São Paulo State), CAPES (Committee for Postgraduate Courses in Higher Education), and CNPq (National Council for Scientific and Technological Development). Siegfried Jaecques gratefully acknowledges funding from the K.U. Leuven research fund (project OT/06/58). The CT-based finite element modeling methods are based on research funded by the EU Framework Programme 5 Quality of Life project QLK6-CT-2002-02442 IMLOAD.

REFERENCES

- Gapski R, Wang HL, Mascarenhas P, Lang NP. Critical review of immediate implant loading. *Clin Oral Implants Res* 2003; 14:515–527.
- Ioannidou E, Doufexi A. Does loading time affect implant survival? A meta-analysis of 1,266 implants. *J Periodontol* 2005; 8:1252–1258.
- Esposito M, Grusovin MG, Willings M, Coulthard P, Worthington HV. Interventions for replacing missing teeth: different times for loading dental implants. *Cochrane Database Syst Rev* 2007; 2:CD003878.
- Schwartz-Arad D, Chaushu G. The ways and wherefores of immediate placement of implants into fresh extraction sites: a literature review. *J Periodontol* 1997; 68:915–923.
- Esposito MA, Koukouloupoulou A, Coulthard P, Worthington HV. Interventions for replacing missing teeth: dental implants in fresh extraction sockets (immediate, immediate-delayed and delayed implants). *Cochrane Database Syst Rev* 2006; 4:CD005968.
- Duyck J, Ronald HJ, Van Oosterwyck H, Naert I, Vander Sloten J, Ellingsen JE. The influence of static and dynamic loading on marginal bone reactions around osseointegrated implants: an animal experimental study. *Clin Oral Implants Res* 2001; 12:207–218.
- Hoshaw SJ, Brunski JB, Cochran GVB. Mechanical loading of Brånemark implants affects interfacial bone modeling and remodeling. *Int J Oral Maxillofac Implants* 1994; 9:345–360.
- Misch CE, Suzuki JB, Misch-Dietsh FM, Bidez MW. A positive correlation between occlusal trauma and peri-implant bone loss: literature support. *Implant Dent* 2005; 14:108–116.
- Isidor F. Loss of osseointegration caused by occlusal load of oral implants. A clinical and radiographic study in monkeys. *Clin Oral Implants Res* 1996; 7:143–152.
- Isidor F. Histological evaluation of periimplant bone at implants subjected to occlusal overload or plaque accumulation. *Clin Oral Implants Res* 1997; 8:1–9.
- Bengazi F, Wennstrom J, Lekholm U. Recession of the soft tissue margin at oral implants. A 2-year longitudinal prospective study. *Clin Oral Implants Res* 1996; 7:303–310.
- Tarnow DP, Magner AW, Fletcher P. The effect of the distance from the contact point to the crest of bone on the presence or absence of the interproximal papilla. *J Periodontol* 1992; 63:995–996.
- Søballe K, Brockstedt-Rasmussen H, Hansen ES, Bünger C. Hydroxyapatite coating modifies implant membrane formation. Controlled micromotion studied in dogs. *Acta Orthop Scand* 1992; 63:128–140.
- Brunski JB. Biomechanical factors affecting the bone-dental implant interface. *Clin Mater* 1992; 10:153–201.
- Brunski JB. Avoid pitfalls of overloading and micromotion of intraosseous implants. *Dent Implantol Update* 1993; 4:77–81.
- Geris L, Andreykiv A, Van Oosterwyck H, et al. Numerical simulation of tissue differentiation around loaded titanium implants in a bone chamber. *J Biomech* 2004; 37:763–769.
- Ekefeld A, Carlsson GE, Borjesson G. Clinical evaluation of single-tooth restorations supported by osseointegrated implants: a retrospective study. *Int J Oral Maxillofac Implants* 1994; 9:179–183.
- Levine RA, Clem DS, Wilson TG Jr, Higginbottom F, Saunders SL. A multicenter retrospective analysis of the ITI implant system used for single-tooth replacements: results of loading for 2 or more years. *Int J Oral Maxillofac Implants* 1999; 14:516–520.
- Schwarz MS. Mechanical complications of dental implants. *Clin Oral Implants Res* 2000; 1:156–158.
- Merz BR, Hunenbart S, Belser UC. Mechanics of the implant-abutment connection: an 8-degree taper compared to a butt joint connection. *Int J Oral Maxillofac Implants* 2000; 15:519–526.
- Behneke A, Behneke N, d'Hoedt B. The longitudinal clinical effectiveness of ITI solid-screw implants in partially edentulous patients: a 5-year follow-up report. *Int J Oral Maxillofac Implants* 2000; 15:633–645.
- Hansson S. A conical implant–abutment interface at the level of the marginal bone improves the distribution of stresses in the supporting bone. *Clin Oral Implants Res* 2003; 14:286–293.
- Hansson S. Implant–abutment interface: biomechanical study of flat top versus conical. *Clin Implant Dent Relat Res* 2000; 2:33–41.

24. Puchades-Roman L, Palmer RM, Palmer PJ, Howe LC, Ide M, Wilson RF. A clinical, radiographic, and microbiologic comparison of Astra Tech and Brånemark single tooth implants. *Clin Implant Dent Relat Res* 2000; 2:78–84.
25. Palmer RM, Palmer PJ, Smith BJ. A 5-year prospective study of Astra single tooth implants. *Clin Oral Implants Res* 2000; 11:179–182.
26. Astrand P, Engquist B, Dahlgren S, Kerstin E, Feldmann H. Astra Tech and Branemark system implants: a 5-year prospective study of marginal bone reactions. *Clin Oral Implants Res* 2004; 15:413–420.
27. Quirynen M, Van Assche N, Botticelli D, Berglundh T. How does the timing of implant placement to extraction affect outcome? *Int J Oral Maxillofac Implants* 2007; 22(Suppl):203–223.
28. Huang HL, Hsu JT, Fuh LJ, Tu MG, Ko CC, Shen YW. Bone stress and interfacial sliding analysis of implant designs on an immediately loaded maxillary implant: a non-linear finite element study. *J Dent* 2008; 36:409–417.
29. Jaecques SVN, Van Oosterwyck H, Muraru L, et al. Individualised, micro CT-based finite element modelling as a tool for biomechanical analysis related to tissue engineering of bone. *Biomaterials* 2004; 25:1683–1696.
30. Geng JP, Tan KB, Liu GR. Application of finite element analysis in implant dentistry: a review of the literature. *J Prosthet Dent* 2001; 85:585–598.
31. Mellal A, Wiskott HWA, Botsis J, Scherrer SS, Belser UC. Stimulating effect of implant loading on surrounding bone. Comparison of three numerical models and validation by in vivo data. *Clin Oral Implants Res* 2004; 15:239–248.
32. Steinemann SG, Mäusli PA, Szmukler-Moncler S, et al. Betatitanium alloy for surgical implants. In: Froes FH, Caplan I, eds. *Titanium '92. Science and technology*. Warrendale, PA: The Minerals, Metals & Materials Society, 1993:2689–2696.
33. Morneburg TR, Proschel PA. Measurement of masticatory forces and implant loads: a methodologic clinical study. *Int J Prosthodont* 2002; 15:20–27.
34. Fontijn-Tekamp FA, Slagter AP, van't Hof MA, Geertman ME, Kalk W. Bite forces with mandibular implant-retained overdentures. *J Dent Res* 1998; 77:1832–1839.
35. Duyck J, Van Oosterwyck H, Vander Sloten J, De Cooman M, Puers R, Naert I. Magnitude and distribution of occlusal forces on oral implants supporting fixed prostheses: an in vivo study. *Clin Oral Implants Res* 2000; 11:465–475.
36. Dar FH, Meakina JR, Aspden RM. Statistical methods in finite element analysis. *J Biomech* 2002; 35:1155–1161.
37. Frost HM. Bone “mass” and the “mechanostat”: a proposal. *Anat Rec* 1987; 219:1–9.
38. Kano SC, Binon PP, Curtis DA. A classification system to measure the implant-abutment microgap. *Int J Oral Maxillofac Implants* 2007; 22:879–885.
39. Palomar AP del, Arruga A, Cegoñino J, Doblaré M. A finite element comparison between the mechanical behaviour of rigid and resilient oral implants with respect to immediate loading. *Comput Methods Biomech Biomed Eng* 2005; 8:45–57.
40. Maeda Y, Satoh T, Sogo M. In vitro differences of stress concentrations for internal and external hex implant–abutment connections: a short communication. *J Oral Rehabil* 2006; 33:75–78.
41. Cehreli MC, Akkocaoglu M, Comert A, Tekdemir I, Akca K. Human ex vivo bone tissue strains around natural teeth vs. immediate oral implants. *Clin Oral Implants Res* 2005; 16:540–548.
42. Claes LE, Heigele CA, Neidlinger-Wilke C, et al. Effects of mechanical factors on the fracture healing process. *Clin Orthop Relat Res* 1998; 355:132–147.
43. Berglundh T, Abrahamsson I, Lang NP, Lindhe J. De novo alveolar bone formation adjacent to endosseous implants. *Clin Oral Implants Res* 2003; 14:251–262.
44. Botticelli D, Berglundh T, Lindhe J. Hard-tissue alterations following immediate implant placement in extraction sites. *J Clin Periodontol* 2004; 31:820–828.
45. Frost HM. Perspectives: bone’s mechanical usage windows. *Bone Miner* 1992; 19:257–271.
46. De Smet E, Jaecques SVN, Jansen JJ, Walboomers F, Vander Sloten J, Naert IE. Effect of constant strain rate, composed by varying amplitude and frequency, of early loading on peri-implant bone (re)modelling. *J Clin Periodontol* 2007; 34:618–624.
47. Forwood MR, Turner CH. The response of rat tibiae to incremental bouts of mechanical loading: a quantum concept for bone formation. *Bone* 1994; 15:603–609.
48. Hsieh YF, Turner CH. Effects of loading frequency on mechanically induced bone formation. *J Bone Miner Res* 2001; 16:918–924.
49. Robling AG, Hinant FM, Burr DB, Turner CH. Improved bone structure and strength after long-term mechanical loading is greatest if loading is separated into short bouts. *J Bone Miner Res* 2002; 17:1545–1554.
50. Rubin CT, McLeod KJ. Promotion of bony ingrowth by frequency-specific, low-amplitude mechanical strain. *Clin Orthop Relat Res* 1984; 298:165–174.
51. Lanyon LE, Rubin CT. Static vs dynamic loads as an influence on bone remodelling. *J Biomech* 1984; 17:897–905.
52. Robling AG, Duijvelaar KM, Geevers JV, Ohashi N, Turner CH. Modulation of appositional and longitudinal bone growth the rat ulna by applied static and dynamic force. *Bone* 2001; 29:105–113.
53. Turner CH. Three rules for bone adaptation to mechanical stimuli. *Bone* 1998; 23:399–407.
54. Vandamme K, Naert I, Geris L, Vander Sloten J, Puers R, Duyck J. The effect of micromotion on the tissue response

- around immediately loaded roughened titanium implants in the rabbit. *Eur J Oral Sci* 2007; 115:21–29.
55. Khraisat A, Stegaroiu R, Nomura S, Miyakawa O. Fatigue resistance of two implant/abutment joint designs. *J Prosthet Dent* 2002; 88:604–610.
56. Sutter F, Weber HP, Sorenson J, Belser U. The new restorative concept of the ITI dental implant system: design and engineering. *Int J Periodontics Restorative Dent* 1993; 13:409–431.
57. Van Oosterwyck H, Duyck J, Vander Sloten J, et al. Patient-dependent FE modeling as a tool for biomechanical optimization of oral reconstruction. In: Middleton J, Jones ML, Shrive NG, Pande GN, eds. *Computer methods in biomechanics and biomedical engineering*. Vol. 3. Amsterdam, the Netherlands: Gordon and Breach Science Publishers, 2001:559–564.

Copyright of Clinical Implant Dentistry & Related Research is the property of Wiley-Blackwell and its content may not be copied or emailed to multiple sites or posted to a listserv without the copyright holder's express written permission. However, users may print, download, or email articles for individual use.